

Technical University of Denmark



## Passivation of a Metal Contact with a Tunneling Layer

**Loozen, X.; Larsen, Jakob Bonne; Dross, F.; Aleman, M.; Bearda, T.; O'Sullivan, B.J.; Gordon, I.; Poortmans, J.; Guy Beaucarne, Jaap Hoornstra, Gunnar Schubert**

*Published in:*  
Energy Procedia

*Link to article, DOI:*  
[10.1016/j.egypro.2012.05.010](https://doi.org/10.1016/j.egypro.2012.05.010)

*Publication date:*  
2011

*Document Version*  
Publisher's PDF, also known as Version of record

[Link back to DTU Orbit](#)

*Citation (APA):*  
Loozen, X., Larsen, J. B., Dross, F., Aleman, M., Bearda, T., O'Sullivan, B. J., ... Guy Beaucarne, J. H. G. S. (2011). Passivation of a Metal Contact with a Tunneling Layer. Energy Procedia, 21, 75-83. DOI: 10.1016/j.egypro.2012.05.010

## DTU Library

Technical Information Center of Denmark

---

### General rights

Copyright and moral rights for the publications made accessible in the public portal are retained by the authors and/or other copyright owners and it is a condition of accessing publications that users recognise and abide by the legal requirements associated with these rights.

- Users may download and print one copy of any publication from the public portal for the purpose of private study or research.
- You may not further distribute the material or use it for any profit-making activity or commercial gain
- You may freely distribute the URL identifying the publication in the public portal

If you believe that this document breaches copyright please contact us providing details, and we will remove access to the work immediately and investigate your claim.

3<sup>rd</sup> Workshop on Metallization for Crystalline Silicon Solar Cells,  
25 – 26 October 2011, Charleroi, Belgium

## Passivation of a Metal Contact with a Tunneling Layer

X. Loozen<sup>a\*</sup>, J. B. Larsen<sup>a,b</sup>, F. Dross<sup>a</sup>, M. Aleman<sup>a</sup>, T. Bearda<sup>a</sup>, B. J. O'Sullivan<sup>a</sup>,  
I. Gordon<sup>a</sup> and J. Poortmans<sup>a</sup>

<sup>a</sup>Interuniversity Microelectronics Center (imec), Kapeldreef 75, 3001 Leuven, Belgium

<sup>b</sup>Technical University of Denmark (DTU), Anker Engélunds Vej 1, 2800 Kgs Lyngby, Denmark

---

### Abstract

The potential of contact passivation for increasing cell performance is indicated by several results reported in the literature. However, scant characterization of the tunneling layers used for that purpose has been reported. In this paper, contact passivation is investigated by insertion of an ultra-thin AlO<sub>x</sub> layer between an n-type emitter and a Ti/Pd/Ag contact. By using a 1.5 nm thick layer, an increase of the minority carrier lifetime by a factor of 2.7 is achieved. Since current-voltage measurements indicate that an ohmic behavior is conserved for AlO<sub>x</sub> layers as thick as 1.5 nm, a 1.5 nm AlO<sub>x</sub> layer is found to be a candidate of choice for contact passivation.

© 2012 Published by Elsevier Ltd. Selection and/or peer review under responsibility of Guy Beaucarne

*Keywords:* Silicon solar cells; Contact passivation; Tunneling layer; Aluminum oxide; MIS contact; PERC

---

---

\* Corresponding author. +32-16-287866; fax: +32-16-281097.

E-mail address: [xavier.loozen@imec.be](mailto:xavier.loozen@imec.be)

## 1. Introduction

Surface passivation is one of the main driving factors for the improvement of the efficiency of silicon solar cells. Most attention throughout the history of photovoltaics has been paid to the passivation of base material and highly-doped silicon areas, but almost no research has been published on the passivation of the metalized areas of silicon solar cells. However, the potential of contact passivation for increasing cell performance is indicated by several results reported in the literature.

By 1984, the highest silicon solar cell efficiency was achieved by using a tunneling SiO<sub>2</sub> layer to passivate the front contacts of a full Aluminum Back Surface Field (BSF) cell [1]. This tunneling layer is approximately 2 nm thick and consists of a thermal oxide grown at 500°C. Unfortunately, no comparison with a cell without contact passivation was made, and investigation of contact passivation has apparently not been pursued by this group.

Later, starting in 1995, the use of an ultra-thin thermal SiO<sub>2</sub> layer (~1.5 nm) under Al contacts is reported by Metz and Hezel [2, 3]. This allows the replacement of the costly front Ti/Pd/Ag contacts by evaporated Al contacts by preventing Al spiking through the POCl<sub>3</sub>-diffused emitter. Such a tunneling SiO<sub>2</sub> layer is regularly integrated in high efficiency Passivated Emitter and Rear Cell (PERC) results published by this group, see e.g. ref. [4]. Recently, an extremely thin (0.24 nm) AlO<sub>x</sub> layer was implemented for the same purpose in PERCs, enabling open-circuit voltage (V<sub>oc</sub>) to reach 673 mV on 0.5 Ωcm p-type Si wafers, i.e. a V<sub>oc</sub> gain of 12 mV compared to cells without AlO<sub>x</sub> tunneling layer [5, 6]. Cousins et al also reported a V<sub>oc</sub> gain of about 32 mV in Interdigitated Back Contact (IBC) cells, enabling the reach of voltages over 720 mV [7]. This gain is said to result mainly from the use of “passivated contacts”. Unfortunately, scant details on the nature of the passivation scheme have been provided, with no mention of a tunnel layer.

All these achievements indicate a real potential of tunneling layers to improve cell performance. Despite this, no in-depth characterization of the passivation process has been published, and it is not clear how much these layers actually reduce interface recombination under metal contacts. In the present work, passivation of metal contacts with tunneling AlO<sub>x</sub> layers is investigated through photoluminescence (PL) and current-voltage (I-V) measurements.

This paper is structured as follows: in section 2, some requirements of a contact passivation layer are discussed, and AlO<sub>x</sub> is proposed as a good candidate for such an application. In section 3, the structure used for minority carrier lifetime investigations is presented, and the impact of AlO<sub>x</sub> as a contact passivating layer is shown through PL measurements. Contact properties of tunnel AlO<sub>x</sub> layers are studied in section 4, and finally, results are discussed in section 5.

## 2. AlO<sub>x</sub> layers as candidate for contact passivation

### 2.1. Passivation of Si by ultra-thin AlO<sub>x</sub> layers

Aluminum oxide has received considerable research attention in the past few years as it was shown to provide excellent *surface* passivation of bulk n- and p-type Si [8-10] as well as highly doped p-type Si [11].

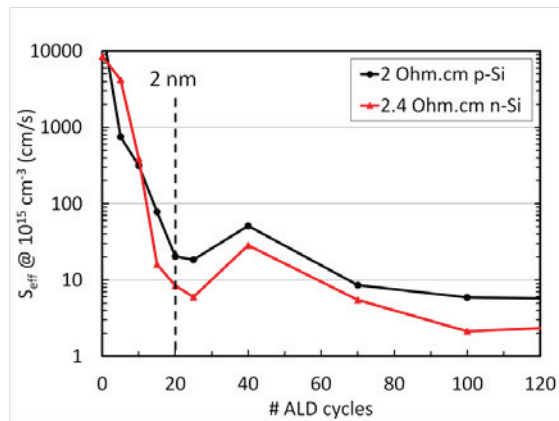


Fig. 1.  $S_{eff}$  as a function of  $\text{AlO}_x$  thickness on p- and n-Si, measured at an excess carrier density of  $10^{15} \text{ cm}^{-3}$ . The  $\text{AlO}_x$  thickness is expressed in amount of ALD cycles, where 1 ALD cycle corresponds to approximately 1 Å, without taking into account the interfacial  $\text{SiO}_x$  possibly present.

The  $\text{AlO}_x$  layers used for that purpose have a thickness generally comprised between 5 and 30 nm, and will be referred to as *thick* layers. However, for *contact* passivation, the passivating layer should be thin enough so that the voltage drop caused by the passage of a few  $\text{A/cm}^2$  (metalized area in the range of the percent of the total area) should not exceed the millivolt range, as otherwise the resistive losses due to the tunneling layer would balance out the gain in  $V_{oc}$  it allows for. Hence, contact passivating layers should be *ultra-thin*, of the order of the nanometer.

For  $\text{AlO}_x$  to be a promising candidate for contact passivation, it should passivate Si when deposited in ultra-thin layers. This has been checked by evaluating the effective surface recombination velocity,  $S_{eff}$ , provided by  $\text{AlO}_x$  layers of various thicknesses in the nanometer range on Si wafers with base doping in the range of  $2.5\text{-}7 \cdot 10^{15} \text{ cm}^{-3}$ . First, n- and p-type polished Float Zone (FZ) Si wafers with resistivity of 2 and  $2.4 \ \Omega\text{cm}$  respectively were cleaned with the following sequence:  $\text{H}_2\text{O}_2\text{:H}_2\text{SO}_4$  1:4 (referred to as SPM clean); HF dip;  $\text{NH}_4\text{OH:H}_2\text{O}_2\text{:H}_2\text{O}$  1:1:5 at  $70^\circ\text{C}$  (SC1); HF dip. Then, they were coated on both sides by  $\text{AlO}_x$  layers deposited by thermal Atomic Layer Deposition (ALD) in a Cambridge NanoTech Savannah tool. Finally, they were submitted to a forming gas anneal (FGA) at  $350^\circ\text{C}$  for 30 min and their effective minority carrier lifetime  $\tau_{eff}$  was measured by Quasi-Steady State Photoconductance. Figure 1 shows the obtained  $S_{eff}$  as a function of the  $\text{AlO}_x$  thickness, where  $S_{eff}$  was evaluated assuming infinite bulk lifetime, i.e.  $S_{eff} = 2W/\tau_{eff}$ , with  $W$  being the substrate thickness. Already with 20 ALD cycles, which correspond to approximately 2 nm  $\text{AlO}_x$ ,  $S_{eff}$  values of 8 and 20 cm/s are achieved on n- and p-Si respectively. Hence, effective passivation of both types of Si with base doping can be reached with ultra-thin layers.

However, to obtain a lowly-resistive ohmic contact, metal contacts are generally deposited on highly-doped surfaces.  $\text{AlO}_x$  has been shown to provide excellent passivation of highly-doped p-type Si [11]. As the target here is passivation of the front contacts in p-type i-PERC cells, passivation of highly-doped n-type regions is investigated in section 2.2.

## 2.2. Passivation of highly doped Si by $\text{AlO}_x$

After receiving an SPM clean followed by an HF dip, lowly doped 280  $\mu\text{m}$  thick polished FZ Si wafers were submitted to  $\text{POCl}_3$  diffusion on both sides. Some of the wafers were subsequently annealed at

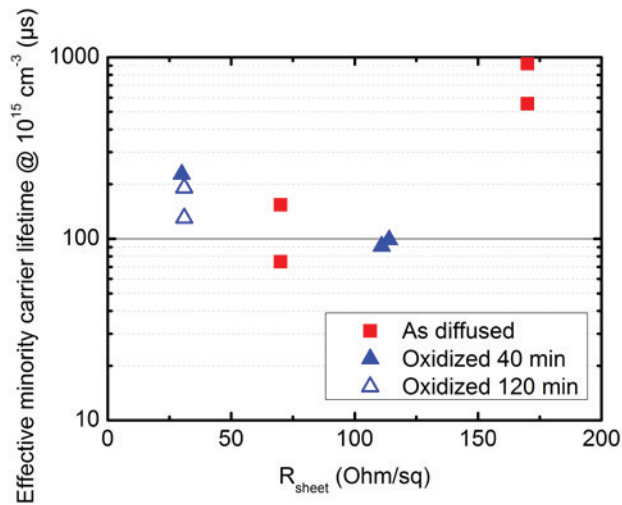


Fig. 2. Lifetime measured on lowly doped FZ Si wafers coated with 30 nm  $\text{AlO}_x$  as a function of the sheet resistance of the underlying  $\text{POCl}_3$  diffused region.

1000°C in oxygen between 40 and 120 min in order to create deep emitters. After removal of the thermal oxide formed, all wafers were coated on both sides by 30 nm thermal ALD  $\text{AlO}_x$ , and submitted to an FGA at 350°C for 30 min. Lifetimes measured on these wafers by QSSPC are plotted as a function of the sheet resistivity  $R_{\text{sheet}}$  in fig. 2. It can be seen that for moderate doping, namely 170  $\Omega/\square$ , lifetimes of the order of 1 ms can be reached. However, for higher doping, namely  $R_{\text{sheet}}$  lower or equal to 115  $\Omega/\square$ , achieved lifetimes are much lower, of the order of 100 to 200  $\mu\text{s}$ .

This strong dependence of surface passivation on  $R_{\text{sheet}}$  can be interpreted by means of the passivation mechanism of  $\text{AlO}_x$ , which relies on field effect [9]. On n-type Si with base doping, the high density of negative charges contained in the  $\text{AlO}_x$  layer and at its interfaces, of the order of  $10^{12}$ - $10^{13} \text{ cm}^{-2}$  [9, 12, 13], is large enough to create a region of strong inversion close to the Si surface. This region of strong inversion results in good surface passivation of lowly doped n-Si, as shown by several authors [9, 10]. For Si with moderate n-type doping, the negatively charged  $\text{AlO}_x$  can still generate a region of weak inversion near the Si surface. This results in some passivation, though less effective than on lowly doped n-Si, as seen in fig. 2 for  $R_{\text{sheet}} \sim 170 \Omega/\square$ . On highly doped n-Si, no or only very weak inversion is achieved, such that passivation is relatively poor, as it is the case for  $R_{\text{sheet}} < 115 \Omega/\square$  in fig. 2.

It has been demonstrated in subsection 2.1 that ultra-thin  $\text{AlO}_x$  layers can offer excellent passivation of lowly doped Si. As contacted surfaces are generally highly doped, the impact of n-type doping level on passivation by thick  $\text{AlO}_x$  was studied in subsection 2.2, and was shown to be strong. In the next section, the passivation achieved with ultra-thin  $\text{AlO}_x$  on 100  $\Omega/\square$  emitters, contacted or not with metal, is

investigated. This doping value is chosen as it is low enough to target high efficiency in PERC-type cells, and high enough to maintain adequate lateral conductivity. For a  $100\Omega/\square$  emitter, fig. 2 tells us that lifetime will be limited to around  $100\ \mu\text{s}$ . Although  $100\ \mu\text{s}$  is a relatively poor value for surface passivation, it is likely much higher than what can be obtained under the contact area of a  $100\ \Omega/\square$  emitter without contact passivation. Besides what is mentioned above, deposition of  $\text{AlO}_x$  by ALD allows for a very precise control, repeatability and reproducibility of the thickness. Consequently,  $\text{AlO}_x$  is a good candidate for contact passivation.

### 3. Lifetime investigation of a metalized area passivated with thin $\text{AlO}_x$ layers

#### 3.1. Structure fabricated for photoluminescence measurements

In this section, the gain in passivation potentially obtained by inserting an ultra-thin  $\text{AlO}_x$  layer under the front contacts of a PERC-type cell is studied. For this purpose, structures resembling PERCs have been fabricated. The starting material is  $180\ \mu\text{m}$  thick Czochralski (CZ) p-Si wafers with a resistivity around  $1.5\ \Omega\text{cm}$ , *the front side textured* and the rear side flat. After an SPM clean and an HF dip, an oxide mask was deposited on the rear side by Chemical Vapor Deposition (CVD) using silane and oxygen as precursor gases. The wafers were cleaned again in an SPM solution and HF dipped and then submitted to  $\text{POCl}_3$  diffusion at  $845^\circ\text{C}$ . Subsequently, the phosphorous glass was removed in diluted HF, and the emitter was submitted to a drive-in at  $860^\circ\text{C}$  for 60 min, to result in a  $90\text{-}100\ \Omega/\square$  emitter. After that, the diffusion mask was removed in concentrated HF, and wafers were cleaned once more in an SPM solution followed by an HF dip. The rear side was passivated by deposition of a  $400\ \text{nm}$  thick CVD oxide layer and a  $160\ \text{nm}$  thick CVD  $\text{SiN}_x$  layer. Wafers were then shortly dipped in HF, and  $\text{AlO}_x$  layers of different thicknesses were deposited by thermal ALD on their front side. To improve passivation offered by the  $\text{AlO}_x$  layers, wafers were annealed in forming gas for 30 min at  $350^\circ\text{C}$ . Immediately before metallization, the wafers were partly dipped in buffered HF for 20 s, in order to selectively remove  $\text{AlO}_x$  from part of the front side of the wafers. Metallization was achieved by e-beam evaporation of a Ti/Pd/Ag stack ( $70\ \text{nm}$  Ti,  $50\ \text{nm}$  Pd and  $1.5\ \mu\text{m}$  Ag) through a shadow mask. The obtained structure is sketched in fig. 3b and 4a: it consists of four different regions, as described in details in fig. 4a. Finally, the lifetime on the different regions of this structure is measured by photoluminescence (PL). The front, textured and metalized side is in contact with the chuck of the PL tool, while laser illumination is applied through the rear, flat and  $\text{SiO}_x\text{-SiN}_x$  passivated side.

A comparison of figs 3a and 3b shows the difference between a PERC and the fabricated structure. First, to allow for the PL laser light to illuminate the wafer and generate free carriers, rear side metallization is suppressed. Second, the front Anti-Reflective Coating (ARC) is omitted, and replaced by the contact passivating layer to be studied. Third, in order to perform comparisons between passivated/unpassivated and metalized/non-metalized areas, the regions coated by  $\text{AlO}_x$  and metal respectively are re-organized. The exact repartition of the layers on the front side is shown in fig. 4a. Comparison between regions I and III shows the impact of the  $\text{AlO}_x$  layer on passivation, i.e. what is actually sought in the experiment. Region IV is necessary for the calibration of the PL measurement by a QSSPC measurement. A comparison between regions III and IV is not straightforward, due to the presence of the metal layer on the front (in contact with the chuck): the quantity measured by PL is the flux of photons resulting from radiative recombination, and a larger fraction of these photons will be reflected on the metalized areas than in the case of the non-metalized ones. Therefore, lifetime of regions I and III might be over-estimated by a factor up to two. As this factor is the same for regions I and III, direct comparison between these two regions is valid. One should however keep in mind that the excess

carrier density at which  $\tau_{eff}$  is measured is different in the different regions, and proportional to  $\tau_{eff}$ . Note that it was verified that patterning of the  $AlO_x$  layer by buffered HF does not lead to any artifact in the PL images, like a change of reflectivity of the passivation layer on the flat side.

### 3.2. Interpretation of the photoluminescence measurements

Fig. 4b shows a photoluminescence image of a structure fabricated with 15 ALD cycles ( $\sim 1.5$  nm  $AlO_x$ ), while fig. 5 shows  $\tau_{eff}$  averaged over areas I, III and IV as a function of  $AlO_x$  thickness. A comparison between regions II and IV in fig. 4b indicates that 1.5 nm  $AlO_x$  does not offer higher passivation of a  $100 \Omega/\square$  P-emitter than native oxide, and the same is true for  $AlO_x$  layers up to 16 nm, as seen in fig. 5. When  $AlO_x$  is replaced by a 90 nm thick passivating  $SiN_x$  ARC in the same structure which is then submitted to firing,  $\tau_{eff}$  is around  $160 \mu s$  in region IV. This difference was verified to be linked to the front side only, the firing of the rear side does not affect  $\tau_{eff}$ .  $AlO_x$  is thus not an effective dielectric for the passivation of n-type emitters with  $R_{sheet} \leq 100 \Omega/\square$ , for the reason discussed in subsection 2.2, and this partly explains the overall relatively low lifetimes obtained in figs 4a and 5. Nevertheless, a clear improvement of the lifetime is observed on metalized areas passivated with  $AlO_x$  layers of 1.5 to 3 nm ( $\tau_{eff} \geq 15 \mu s$ ), as compared to unpassivated metalized areas ( $\tau_{eff} \leq 7.5 \mu s$ ). In the 1.5-2 nm range, contact passivation by  $AlO_x$  leads to an increase of lifetime by a factor of almost 3.

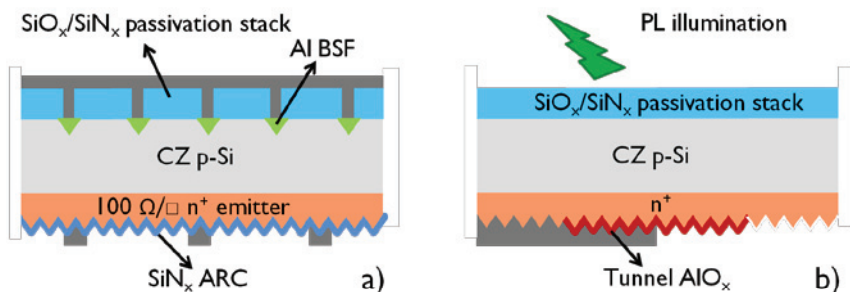


Fig. 3. Schematic drawings of a) a PERC-type cell with rear side facing up, and b) the structure fabricated for investigating contact passivation in PERC-type cells.

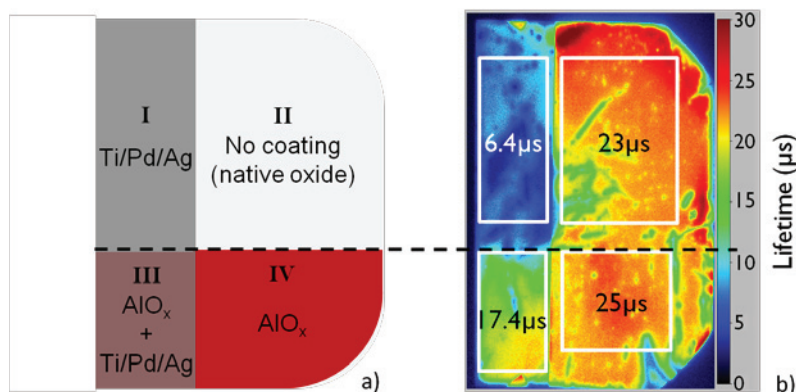


Fig. 4. a) schematic drawing of the structure fabricated for PL measurements, with the four regions with different coatings labeled I to IV. b) the same structure seen by PL, with a  $\sim 1.5$  nm thick  $AlO_x$  layer (deposited via 15 ALD cycles). Lifetime averaged over the white rectangular areas is indicated. The excess carrier density on the non-metalized areas is  $5.10^{14} \text{ cm}^{-3}$ ; the one under the metalized is lower, and proportional to the lifetime. The dashed line separates  $AlO_x$  coated and non-coated areas.

Lifetime measurements by PL have shown that ultra-thin  $\text{AlO}_x$  layers can provide a certain level of contact passivation. In order to find potential applications into solar cells, these passivating layers must not affect contact properties too strongly. Checking this is the subject of next section.

#### 4. Contact properties of passivating $\text{AlO}_x$ tunnel layers

Contact properties of Ti/Pd/Ag stacks with an underlying  $\text{AlO}_x$  layer were studied on flat and textured emitters. The structure used with flat emitters is shown in fig. 6a, and fabricated as follows: after an SPM clean and an HF dip, a  $120 \Omega/\square$  n-type emitter is obtained by  $\text{POCl}_3$  diffusion on p-type wafers, with a process similar to the one described in subsection 3.1. The emitter is then coated with an ultra-thin  $\text{AlO}_x$  layer, on which circular Ti/Pd/Ag contacts with a diameter of  $500 \mu\text{m}$  are evaporated through a shadow mask. The ohmic nature of the Metal-Insulator-Silicon (MIS) contacts formed that way is verified by

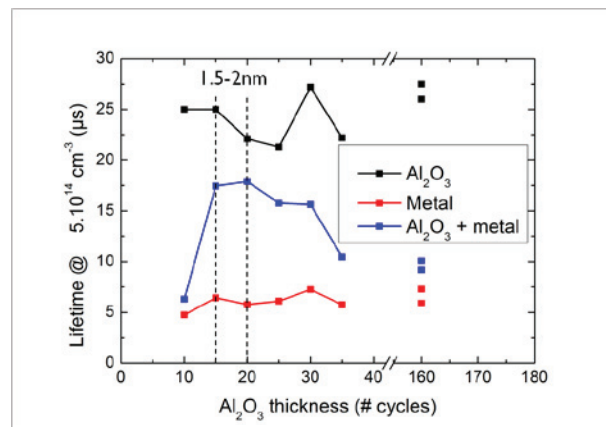


Fig. 5. Averaged value of  $\tau_{eff}$  over regions I, III and IV of fig. 4a, as a function of  $\text{AlO}_x$  thickness. One ALD cycle corresponds to about  $1 \text{ \AA}$ .

measuring the current-voltage (I-V) characteristics between adjacent dots. For  $\text{AlO}_x$  layers with a thickness larger than or equal to 2 nm, weak to strong deviation from an ohmic behavior were observed, and an example is shown in fig. 6b for a 2 nm thick layer. Interestingly, for  $\text{AlO}_x$  thicknesses less than or equal to 1.5 nm, ohmic behavior was observed. This is an important observation, since the highest lifetimes obtained in the previous section were achieved with 1.5 and 2 nm thick layers. Consequently, a 1.5 nm  $\text{AlO}_x$  layer deposited between a  $\text{POCl}_3$  emitter in the  $100\text{--}120 \Omega/\square$  range and a Ti/Pd/Ag contact provides a significant increase of lifetime *without* notably affecting the ohmic nature of this contact.

A similar experiment was repeated with textured  $100 \Omega/\square$   $\text{POCl}_3$  emitters. All structures with  $\text{AlO}_x$  layers with a thickness ranging from 1 to 16 nm were found to have ohmic contacts. This is very surprising, as one would expect layers above 4 nm to be insulating. A possible explanation is that the electrical field is strongly increased at the pyramid tips by tip effect, leading to a local breakdown of the  $\text{AlO}_x$  layer. In that case, the current would flow through the pyramid tips only. This hypothesis remains to be verified.



## 5. Summary and conclusion

The potential of contact passivation for increasing cell performance is indicated by several results reported in the literature. However, scant characterization of the tunneling layers used for that purpose has been reported. In the present paper, tunneling  $\text{AlO}_x$  layers are characterized through lifetime and I-V measurements. It is first demonstrated that ultra-thin  $\text{AlO}_x$  layers can effectively passivate p- and n-Si with base doping. It is then shown that passivation by  $\text{AlO}_x$  is less efficient on highly-doped n-Si surfaces. This partly explains the overall low lifetimes obtained on the structures fabricated to compare lifetimes under passivated and non-passivated metalized areas. Also the quality of the bulk and of the surface passivation on the non-metalized side could be the origin of the low lifetimes, such that the achieved results should be confirmed by using higher quality substrates and excellent surface passivation on the rear side.

Nevertheless, an increase in minority carrier lifetime by a factor of two to three by insertion of an ultra-thin  $\text{AlO}_x$  layer under a Ti/Pd/Ag-metalized area has been achieved, with highest lifetime values seen for 1.5-2 nm thick layers. I-V measurements on flat emitters have shown that an ohmic behavior is conserved for  $\text{AlO}_x$  layers as thick as 1.5 nm.

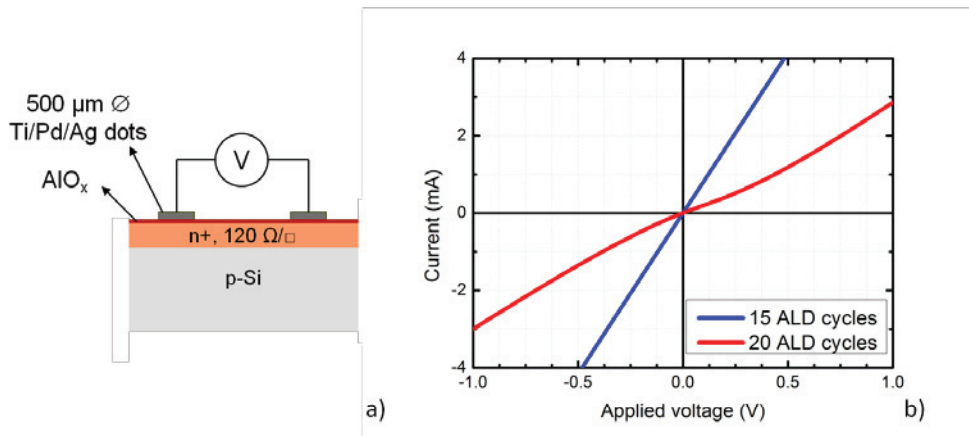


Fig. 6. a) Schematic drawing of the structure used to measure contact properties on flat emitters. b) I-V curves measured on the structure shown in a) for  $\text{AlO}_x$  layers deposited with 15 or 20 ALD cycles (~1.5 or 2 nm  $\text{AlO}_x$ ).

As a consequence, a 1.5 nm  $\text{AlO}_x$  layer exhibits the requirements necessary for contact passivation on an n-type emitter: it leads to a significant improvement of lifetime under a metal contact without notably affecting the ohmic nature of this contact.

## References

- [1] Green MA, Blakers AW, Shi J, Keller EM, Wenham SR. High-efficiency silicon solar cells. *IEEE Trans. Electron Devices* 1984;**ED-31**:679-683.
- [2] Metz A, Hezel R. Record efficiencies above 21% for MIS-contacted diffused junction silicon solar cells. *Proceedings of the 26<sup>th</sup> IEEE Photovoltaic Specialist Conference* 1997:283-6.
- [3] Hezel R, Metz A. Crystalline silicon solar cells with efficiencies above 20% suitable for mass production. *Proceedings of the 16<sup>th</sup> European Photovoltaic Solar Energy Conference* 2000:1091-4.
- [4] Schmidt J, Merkle A, Brendel R, Hoex B, van de Sanden MCM, Kessels WMM. Surface passivation of high-efficiency silicon solar cells by atomic-layer-deposited Al<sub>2</sub>O<sub>3</sub>. *Prog. Photovolt.* 2008;**16**:461-6.
- [5] Zielke D, Petermann JH, Werner F, Veith B, Brendel R, Schmidt J. Contact passivation in silicon solar cells using atomic-layer-deposited aluminum oxide layers. *Phys. Status Solidi RRL* 2011;**5**:298-300.
- [6] Petermann JH, Zielke D, Schmidt J, Haase F, Rojas EG, Brendel R. 19% - efficient and 43μm - thick crystalline Si solar cell from layer transfer using porous silicon. *Prog. Photovolt.: Res. Appl.* 2011;**20**:1-5.
- [7] Cousins PJ, Smith DD, Luan H-C, Manning J, Dennis TD, Waldhauer A, Wilson KE, Harley G, Mulligan WP. Generation 3: improved performance at lower cost. *Proceedings of the 33<sup>rd</sup> IEEE Photovoltaic Specialist Conference* 2010:275-8.
- [8] Agostinelli G, Delabie A, Vitanov P, Alexieva Z, Dekkers HFW, De Wolf S, Beaucarne G. Very low surface recombination velocities on p-type silicon wafers passivated with a dielectric with fixed negative charge. *Sol. Energy Mater. Sol. Cells* 2006;**90**:3438-43.
- [9] Hoex B, Schmidt J, Pohl P, van de Sanden MCM, Kessels WMM. Silicon surface passivation by atomic layer deposited Al<sub>2</sub>O<sub>3</sub>. *J. Appl. Phys.* 2008;**104**:044903.
- [10] Dingemans G, Seguin R, Engelhart P, van de Sanden MCM, Kessels WMM. Silicon surface passivation by ultrathin Al<sub>2</sub>O<sub>3</sub> films synthesized by thermal and plasma atomic layer deposition. *Phys. Status Solidi RRL* 2010;**4**:10-2.
- [11] Hoex B, Schmidt J, Bock R, Altermatt PP, van de Sanden MCM, Kessels WMM. Excellent passivation of highly doped p-type Si surfaces by the negative-charge-dielectric Al<sub>2</sub>O<sub>3</sub>. *Appl. Phys. Lett.* 2007;**91**:112107.
- [12] Rothschild A, Vermang B, Goverde H. Atomic layer deposition of Al<sub>2</sub>O<sub>3</sub> for industrial local Al back-surface field (BSF) solar cells. *Photovolt. International* 2011;**13**:92-101.
- [13] Saint-Cast P, Kania D, Hofmann M, Benick J, Rentsch J, Preu R. Very low surface recombination velocity on p-type c-Si by high-rate plasma-deposited aluminum oxide. *Appl. Phys. Lett.* 2009;**95**:151502.